Structure-property relationships in glass reinforced polyamide: 3) Effects of hydrolysis ageing on the dimensional stability and performance of short glass-fibre reinforced Polyamide 66.

J. L. Thomason

Abstract

We present results on an in-depth study of the effects of hydrolysis testing on the mechanical performance, weight change, and dimensional stability of injection moulded glass-fibre reinforced polyamide 66 based on two chopped fibre products with different sizing formulations. Composite and resin samples have been characterised both dry as moulded and after conditioning at either 120°C or 150°C for a range of times up to 1000 hours. The results reveal that hydrothermal ageing in water-glycol mixtures results in significant changes in the mechanical performance, weight, and dimensions of these materials. The negative effects of conditioning could be mitigated to some degree by the appropriate choice of the glass fibre sizing; however the sizing effect diminished with increasing conditioning time. All materials showed a weight increase due to conditioning at 120°C which was typical of a single Fickian diffusion process and there was clear evidence of multiple processes involved when conditioning at 150°C. It was not apparent that the glass fibre sizing affected the dimensional stability of the composites. We show that there is a strong correlation between the swelling of these samples and the level of fluid adsorption. Although the PA66 resin showed reasonably homogeneous swelling, the composites exhibited different levels of swelling depending on direction. These effects were well in line with the known effects of fibres on restriction of the matrix deformation (mechanical, thermal or moisture swelling) in the fibre direction. These differences correlate well with the average fibre orientation with respect to the various direction axes. Composite tensile strength and unnotched impact resistance appeared to scale inversely with the level of swelling of the material.

Polymer Composites, **28**, (3), 344-354, Wiley InterScience Ltd, June 2007

Introduction

Glass fibre reinforced polyamides, such as nylon 6 and nylon 66, are excellent composite materials in terms of their high levels of mechanical performance and temperature resistance. However, the mechanical properties of polyamide based composites decrease markedly upon absorption of water and other polar fluids. The mechanical performance of these composites results from a combination of the fibre and matrix properties and the ability to transfer stresses across the fibre-matrix interface. Variables such as the fibre content, diameter, orientation and the interfacial strength are of prime importance to the final balance of properties exhibited by injection moulded thermoplastic composites (1-5). The optimization of composite processibility and performance through control of the base materials and the various steps of fibre-matrix combination and parts production is already a major technical challenge. The challenge to a fibre reinforcement supplier is how to offer outstanding reinforcement products which can meet the demands of all the intermediaries in the composite chain and match the internal manufacturing and financial targets.

Short fibre reinforced thermoplastics have been used in the automotive industry for many years and there has recently been a strong growth in the use of polyamide based materials in under-the-hood applications (6). These applications place stringent requirements on such materials in terms of dimensional stability and mechanical, temperature and chemical resistance. There has been a rapid increase in the number of moulded composites exposed to engine coolant at high temperatures and this has led to a need for an improvement in our understanding of the performance of glass-reinforced-polyamide under such conditions. Typical testing for these applications involves measurement of mechanical properties before and after conditioning of the test material in model coolant fluids for a fixed time, up to 1000 hours, at temperatures in the 100-150°C range. It is not always easy to obtain a good understanding of the structure-performance relationships of a material from such snapshots of performance taken at a single condition. However, it has been known for sometime within the industry that the chemical nature of the glass fibre sizing can have a strong influence on the retention of some mechanical properties of composites exposed to such hydrothermal conditioning. It is also well known that polyamide materials absorb relatively high levels of moisture when exposed to hydrothermal conditioning in water and that this can cause significant dimensional changes (7-13). Despite this, and the fact that such hydrothermal testing has become commonplace for under-the-hood applications, there has been little systematic investigation of dimensional change of glass-fibre reinforced polyamide composites during such conditioning in coolant fluid.

In this report we present the results of such a systematic study of the changes of dimension and mechanical performance of injection moulded glass reinforced polyamide 66 composites during hydrothermal conditioning in model coolant fluid. Composites have been prepared using two chopped glass products where one contains a sizing system which has been optimised to improve the performance of composites subjected to hydrothermal treatments. The experiments have been carried out at 120°C and 150°C for a range of conditioning times up to1000 hours. The results for composite mechanical performance have been analysed using available micro-mechanical models and correlated with the measured changes in weight and dimensions.

Experimental

The fibres used in this study, 173X-10C and 123D-10C, were all produced using the Owens Corning Cratec® process for chopped strands using E-glass. These samples were chopped to a length of 4 mm and the individual fibres had a nominal average diameter of 10 μm. Both samples were coated with sizings which are designed for polyamide reinforcement. 123D is a typical sizing designed to maximise the "dry as moulded" (DaM) performance of glass reinforced polyamides where the main ingredients are aminosilane coupling agent and a commercial polyurethane dispersion (14,15). 173X sizing contains some extra components, including the homopolymer of an acrylic acid monomer, which enhance the retention of composite mechanical properties in elevated temperature hydrolytic environments (16,17). The polyamide 6,6 (PA6,6) used was DuPont Zytel 101. The glass bundles and pre-dried PA6,6 pellets were dry blended by weight to a nominal 30% w/w glass content and compounded on a single screw extruder (2.5 inch, 3.75:1, 24:1 L/D screw). The compounds were moulded into test bars on a 200-ton Cincinnati Milacron moulding machine. Set point temperatures were 288-293°C for compounding and 293-299°C for moulding, at a mould temperature of 93°C. Three series of samples were moulded, series A using 123D-10C glass, series B using 173X-10C glass, and series R containing only the PA6,6 resin. Hydrolysis conditioning took place in a temperature controlled self-pressurized vessel with samples fully immersed in a 50:50 mixture of water and glycol at either 120°C or 150°C. On removal from conditioning container samples were cooled to room temperature in a bath of 50/50 water/glycol, weighed and measured, and then stored in plastic bags for immediate mechanical testing. It was found that the resin only samples were too physically degraded by the conditioning at 150°C to be able to make any reliable measurements. Tensile properties were measured in accordance with the procedures in ASTM D-638, using ASTM Type I specimens at a crosshead rate of 5 mm/min (0.2 inches/min) and an extensometer gauge length of 50 mm (2 inches). Izod and modified Charpy impact properties were measured on ten specimens in accordance with the procedures in ASTM D-256 and ASTM D-4812. Unless otherwise stated, all mechanical property testing was performed at 23°C and at a relative humidity of 50%. Fibre length and diameters were determined by image analysis and optical microscopy on fibre samples removed from the moulded bars after high temperature ashing to determine the composite fibre content. Results are given in Table 1.

Results

Moisture absorption related processes in polymers and composites are normally analysed against the square root of exposure time (18,19) and we have followed this procedure in the Figures which are presented here. Error bars in these Figures represent the 95% confidence interval on the average value presented. The tensile modulus of the 120°C hydrolysed composite samples shown in Figure 1 is similar up to 96 hours, showing an initial sharp drop to approximately 45% of the DaM level (of 9.7 Gpa). After 96 hours conditioning treatment a difference in performance between samples A and B is observed with sample B continuing a slow increase in tensile modulus, recovering to 55% of the DaM level by 1000 hours. Sample A shows a relatively flat performance at times greater than 96 hours, resulting in a slightly lower overall performance than sample B. The resin sample shows a much greater initial drop in performance, losing 80% of the DaM tensile modulus in the first 24 hours of treatment, after that the tensile modulus of the resin remains approximately constant out to 1000 hours hydrolysis time. Treatment at 150 °C causes a similar level of tensile modulus loss in the first 24 hours for samples A and B. At longer times the tensile modulus of sample A continues to drop to about 35% of the DaM level whereas sample B remains approximately constant at 45% of the DaM performance.

The tensile strength trends shown in Figure 2 are somewhat different from the tensile modulus results. For conditioning at 120°C the tensile strength falls 50%, from a DaM value of 177 MPa, during the first 24 hours. At longer exposure times sample A continues a slow fall in tensile strength reaching 35% of DaM by 1000 hours. In contrast, sample B shows an increase in tensile strength after the initial drop, recovering to 57% of the DaM value after 7 days. At times greater than 7 days sample B also shows a very slow loss in tensile strength reducing to 53% of DaM by 1000 hours. The resin sample shows the same large drop in tensile strength during the first 24 hours followed by essentially unchanged performance at longer conditioning times. At 150°C the initial drop after 24 hours is similar for sample B, however sample A shows an even greater initial drop down to 33% of the DaM level. The further drop in tensile strength with longer conditioning times is much faster at 150°C although sample B maintains higher levels of tensile strength until approximately 600 hours exposure. The tensile elongation after hydrolysis is shown in Figure 3 where the y-axis is a logarithmic scale. It can be seen that the tensile elongation of the resin increases fivefold in the first 24 hours of conditioning at 120°C. At longer times the tensile elongation shows a slow decrease with increasing conditioning time but still maintains a twofold increase at 1000 hours. The composite samples appear to follow a similar trend at 120°C with sample B reaching a somewhat higher level of tensile elongation than sample A and then both samples follow a fairly parallel decrease with greater exposure times. The trends at 150°C are similar but with the changes taking place more rapidly and the decrease in tensile elongation at longer times being much greater than at 120°C. Whereas, at 120°C the composites have approximately the same tensile elongation at 1000 hours treatment compared with the DaM performance, at 150°C the composites maintain less than 10% of the DaM tensile elongation after 1000 hours treatment.

The results for Izod and Charpy Unnotched impact strength are presented in Figures 4 and 5. It is interesting to note that, despite the fact that there is no significant difference between

the DaM impact performance of samples A and B, glass B gives systematically higher unnotched Izod impact once the hydrolysis process has been started. At 120°C sample B shows an initial increase in unnotched Izod impact with a maximum around 72 hours after which there is a slow reduction with increasing time. Conversely sample A shows an initial drop in unnotched Izod impact which reaches an approximately constant level after the first 72 hours of the treatment. The resin sample also exhibits a steep drop in unnotched Izod impact during the initial phase of the treatment reaching a minimum of 40% of the DaM value at about 96 hours. After this time there appears to be a slow increase in unnotched Izod impact of the resin with treatment time. At 150°C sample A loses 50% unnotched Izod impact after only 48 hours and continues a steep drop in performance until reaching approximately 15% at 9 days after which a slow continual drop in unnotched Izod impact continues. Sample B also shows a steep drop in performance in the first 9 days but maintains a higher unnotched Izod impact level than sample A. No mechanical data could be obtained on resin sample due to a high level of physical degradation. The unnotched Charpy impact performance of these samples followed similar trends to the unnotched Izod impact although with some differences in absolute levels. At 120°C both sample A and B show a sharp increase in unnotched Charpy impact after 24 hours treatment followed by a gradual decline over the rest of the 1000 hours treatment time. Sample B reaches a significantly higher maximum value than sample A after which the two 120°C lines in Figure 5 run approximately in parallel. In contrast the resin sample shows a steep decline in unnotched Charpy impact after 24 hours treatment after which the performance remains approximately constant. At 150°C treatment temperature sample B shows a much lower increase in unnotched Charpy impact at 24 hours than at 120°C, after which the decline in performance is much quicker and proceeds to much lower levels. Sample A shows no initial increase in performance only a steep decline, ultimately to approximately the same very low level of unnotched Charpy impact (5% of DaM value) at longer treatment times.

Water absorption in polymers and composites is normally analysed against the square root of exposure time to enable the use of standard diffusion models (18,19). Figure 6 shows such a plot of percentage increase in sample weight of both tensile dogbone and impact bars for composites A and B and the resin only sample after hydrolysis at 120°C. The data appears to show typical Fickian diffusion with a rapid initial uptake of liquid followed by a slow approach to an equilibrium absorption level. It is interesting to note that, at the first data point at 24 hours, we have already reached >75% of the final equilibrium level which is indicative of the very rapid diffusion of liquid into these polyamide based samples. Unfortunately this result then precludes the use of Fickian analysis to calculate diffusion coefficients which requires obtaining the slope of the initial part of the plot which should be linear. At 24 hours exposure we are clearly already past the linear part of the curve. It seems reasonable to assume that the glass fibres do not account for any of the weight increase seen during the hydrolysis treatment. We have therefore also shown the calculated expected weight increase of the composite samples based on their resin content and the weight increase samples for the resin only sample. It can be seen that the composites absorb significantly less fluid compared to the expectation based on the resin results. It is clear that this is not due to time dependent effects since both resin and composite samples have clearly reached equilibrium after 9 days exposure. Apparently the presence of the glass fibres reduces the ability of the polyamide resin to absorb the level of fluid that is absorbed by the resin in an unrestrained environment. It can also be seen in Figure 6 that there is no

significant difference between the absorption results obtained with the tensile and impact bars. This was found to be the case in all of the absorption and dimensional change data and we have therefore averaged the values from the two test specimen types in the subsequent Figures. Figure 7 compares the weight increase of sample A and B after hydrolysis at 150°C and 120°C. It can be seen that both samples absorb significantly higher levels of fluid when treated at higher temperature. Furthermore, whereas the results at 120°C appear to follow a single diffusion process, at 150°C there appears to be some evidence of more structure in the curves. There appears to be a step up in absorption after 72 hours exposure and again after 600 hours. Using the paired T-test to compare the performance of sample A and B we can state that, at the 95% confidence level, sample B adsorbs less fluid that sample A at both conditioning temperatures.

The results for the change in width and thickness of the injection moulded bars as a function of conditioning time and temperature are shown in Figures 8 and 9. The curves in Figure 8 for samples hydrolysed at 120°C follow similar trends as the weight increase data in Figure 6. It should be noted that the thickness of the composite samples appears to increase significantly more than the width. To a lesser extent this is also true for the resin sample. Furthermore, despite the reduced resin content of the composites, the swelling of the composite and resin bars is approximately equal in the thickness. The resin swells significantly more than the composites in the width. The swelling of these samples at 150°C also follows very similar trends to the liquid uptake data. In this case the difference between the swelling in the thickness and width directions is even greater than observed at 120°C conditioning temperature. Indeed the swelling in the width direction increased by approximately 50% above the 120°C samples whereas the swelling in the thickness direction more than doubles at 150°C compared to 120°C. It is also notable that the structure in the curves for thickness swelling at 150°C is very similar to that observed in the fluid uptake data in Figure 7 with “steps” apparent at 72 hours and 600 hours. There is no obvious trend in these data with respect to the relative performance in swelling of samples A and B. In Figure 10 we have combined the length and width data to obtain the change in sample cross section. It can be seen that conditioning at 150°C leads to an approximately doubling of the composite cross section compared to 120°C at equal conditioning time. There is no significant difference between samples A and B at 150°C or 120°C in Figure 10. However, at 120°C the resin sample has a larger change in cross section than the composites.

Discussion

The elastic behaviour of composite materials is often considered in terms of deformations caused by mechanical stresses due to physically applied loads such as presented in Figures 1-3. However, deformations are also produced by environmental changes such as temperature changes and moisture absorption. The relevant physical parameters which quantify these phenomena are the coefficients of thermal expansion (CTE) and the coefficients of swelling. Although CTE's are the more familiar of these coefficients, these two phenomena are similar and can be treated in a similar fashion. The swelling coefficient (β) is defined as $\beta=\varepsilon/C$ where $\varepsilon=\delta L/L$ the swelling strain in any direction and $C=\delta W/W$ the mass of absorbed moisture per unit mass (20).

It seems clear from the results presented above that, as predicted, there is a strong correlation between the weight increase of these samples and their dimensional change during hydrolysis treatment. In Figure 11 we show the data for ε versus C for the composites width and thickness at both conditioning temperatures. It can be seen that we obtain excellent linear relationships for the change in these dimensions for both composite samples. The solid lines in Figure 11 are the least squares fitted lines for the 120°C data and it can be seen that the extrapolation of these lines also fits well with the initial data obtained at 150°C. From the slope of these lines we obtain values of β of 0.38 for the width and 0.85 for the thickness. It is interesting to note that the deviations from these lines in Figure 11 appears to occur after the occurrence of the first "step increase" in the moisture absorption observed in Figure 7 for the 150°C conditioning. This may well be indicative of a second mechanism governing the changes in these samples due to the hydrothermal conditioning. The directional dependence of CTE's in fibre reinforced composites is well known and is attributed to the restriction of expansion in the fibre direction due to the much lower CTE of the fibre compared to the polymer matrix (21,22). In a similar fashion we assume that $\beta=0$ for glass fibres and so the presence of fibres will restrict the swelling in the fibre direction and consequently increase the matrix swell normal to the fibre direction due to Poisson's effects in the matrix. There is little degree of out of plane fibre orientation (through the thickness) in these injection moulded samples and consequently we observe a higher swell in the thickness as compared to the width where the fibres in the "core" of the moulding have a somewhat more random in-plane orientation. Since the highest level of fibre orientation is in the flow direction in the mould we would have expected very low levels of swell in the length direction of these samples had we been able to measure it. It is interesting to note that we also observe some differences in β for the moulded resin samples. The value of 0.28 in the width versus 0.37 in the thickness direction for the resin may well be indicative of some orientation at the molecular level in the injection moulded polyamide polymer.

In Figure 12 we combine the width and thickness data to examine the change in sample cross section versus the level of adsorbed moisture. It can be seen that nearly all of the composite data appear to lie on the same line. It is also clear that the data for the resin sample (R120) lies well below the trend-line for the composites. One of the likely reasons for this difference is due to the fact that we have only measured the dimension changes of the injection moulded bars in two directions. If we now assume that the dimensional change

in the length of the resin bars is unaffected by any possible anisotropy in molecular orientation then we can use an average value of the dimensional change in the width and thickness (7%) to obtain an estimate of the volumetric dimensional change of the resin samples. This data (R120*) is also shown in Figure 12. It can be seen that this data is substantially closer to a relationship of dimensional change equal to weight increase although the slope of the line is now slightly more than unity. However, this small difference can be explained by the density difference between the polyamide resin and the absorbed fluid. It is easily shown that the slope of the line, for the resin sample, shown in Figure 12 must also be modified by the ρ_R/ρ_A the densities of the polyamide resin and absorbed fluid. Although we cannot be sure that the polymer absorbs fluid containing the same ratio of water/glycol as is present in the treatment bath, by using a value of ρ_A =1.07 and ρ_R=1.14 we obtain an expected slope =1.065, which is almost exactly the value of the slope of the line shown in Figure 12. We can therefore state that within the experimental error and the assumptions given above that the dimensional change of the polyamide resin is exactly explained by the amount of fluid which the sample absorbs.

Following similar arguments to those presented above for the resin sample it is also easily shown that, if the matrix resin in the composites swells by the exactly expected volume of the absorbed liquid, then we should obtain a slope of ρ_C/ρ_A for the composite data in Figure 12. However, in this case we cannot make simple assumptions about the dimensional change of the composites in the length direction. Dimensional change of composites due to fluid absorption follows similar trends as dimension change due to temperature change. It is well known that the much lower thermal expansion coefficient of glass fibres, compared to the polymer matrix, leads to restriction of the linear thermal expansion of composites in the fibre direction and an increase in the linear thermal expansion coefficient normal to the fibre direction (21,22). Similar trends can be expected from the swelling of the composites being discussed here since we assume that the fibres show no dimensional change in these experiments. Thomason (22) showed clear evidence for the anisotropy of the coefficients of linear thermal expansion in a detailed study of random in-plane glass fibre reinforced polypropylene. The fibre orientation pattern in an injection moulded bar is much more complicated, however the majority of the fibres can also be expected to be oriented in-plane, with a greater proportion oriented in the flow (injection) direction and a smaller fraction oriented normal to the flow direction. Such an orientation pattern would therefore lead us to expect a greater than average (compared to a resin value normalised by glass content) swell in the composite thickness, and we would expect a significantly reduced swell in the flow (length) direction. Expectations for swelling in the width direction would fall somewhere in between these two. Examination of the width and thickness dimensional change data in Figure 8 is fully in line with the above discussion. The composite swell in thickness is much greater than that expected from a glass content normalised resin value, whereas swelling in the width is approximately equal to the value expected from the normalised resin value. We would therefore expect that the change in composite length would be significantly less than the 4-5% expected from a glass content normalised resin value.

We can obtain an estimation of the length change in these samples from the data in Figure 12. An average density for these composite samples is ρ_C =1.38 g/cc which would result in a line with a slope of 1.29 in Figure 12 if the y-axis was volumetric dimensional change and the composite volume increased by an amount exactly equal to the volume of absorbed

fluid. The least squares fitted value for the 120°C composite data in Figure 12, where the y-axis is cross section dimensional change, is 1.20. It would therefore require a length swelling coefficient of only 0.09 to adjust the dimension change to volumetric and obtain the required slope. This would convert to a length change of approximately 1% at equilibrium during 120°C conditioning. The expected volumetric swelling coefficient of 1.29 converts to a linear swelling coefficient of 0.43 for homogeneous expansion of the material. Comparing this with the values in Figure 11 we confirm again the reduction of swell in the width and increase in the thickness due to the presence of fibres in the composites.

In order to test this hypothesis on the low level of change in composite length during conditioning we have carried out some dimensional change measurements in an ongoing series of experiments on long fibre reinforced PA66 (23). We have measured weight and all three dimension changes in samples conditioned in water/glycol mixtures at 120°C for 168 and 600 hours. Samples included Zytel 101 PA66 resin and system A composites. The results for the various swelling coefficients are summarised in Table 2. We find excellent agreement for the width and thickness changes between the new data and the data in the previous Figures. It is also quite clear from the data in Table 2 that the change in composite length during conditioning is extremely low (much lower than the estimate of 1% given above). Taking the average of the four composite data points available for each dimension we get swelling coefficients of 0.33 for width and 0.86 for thickness (in excellent agreement with previous values) and only 0.03 for length. Interestingly, the average values of swelling coefficient for the resin only samples (width=0.29, length=0.26, thickness=0.42) also indicate the same heterogeneity in the swelling of the resin samples observed in the previous data.

We have previously discussed in some detail (4,5) the common approaches to analysing data for the composite tensile modulus using simple "rule-of-mixtures" techniques. One approach based on the Cox shear lag analysis uses the following equation to calculate composite modulus E_c from the moduli of the two components.

$$E_c = \eta_0 \eta_l V_f E_f + (1 - V_f) E_m \qquad (1)$$

where E_f is the fibre modulus, E_m is the matrix modulus, V_f is the fibre volume fraction, If the fibre length is known then the modifying factor η_l can be calculated using the Cox shear lag method (24). Combining these values with the experimental values of composite and matrix modulus we can obtain a value for the orientation parameter (η_o) for each sample at any condition.

Another approach is to use the equation

$$E_c = \eta_0 E_1 + (1 - \eta_0) E_2 \qquad (2)$$

where E_1 and E_2 are obtained from the Halpin-Tsai equations (25) for the modulus of a unidirectionally reinforced laminate.

$$E_j = E_m\left[\frac{1+\xi_j \eta_j V_f}{1-\eta_j V_f}\right] \qquad \eta_j = \frac{\left(E_f/E_m\right)-1}{\left(E_f/E_m\right)+\xi_j} \qquad \xi_1 = \frac{2L}{D} \qquad \xi_2 = 2 \qquad (3)$$

A test of the validity of the above models for analysis of hydrolysed samples is to use both approaches to calculate and compare the values of η_o . In the case of the hydrolysed samples it is necessary to adjust the DaM measured value of composite fibre weight fraction and matrix density for the absorption of fluid during the treatment. Clearly it is also necessary to use the values for the stiffness of the resin after treatment, for this reason we have only been able to carry out this analysis for the conditioning at 120°C.

Figure 13 shows the average fibre orientation data calculated using the two methods discussed above for samples A and B as a function of hydrolysis time at 120°C. It can be seen that the two methods give values in good agreement for the DaM case. However, after hydrolysis the two methods give divergent trends for the average orientation factor. The Cox analysis indicates a small drop in η_o in the early stages of the treatment. From the results shown in Figures 6-8 we know that we are only close to equilibrium at treatment times greater than 200 hours. It may be that there are some significant differences in the diffusion of fluid into the composites matrix as opposed to the resin only sample in the initial period of conditioning. For this reason we should be careful of drawing any definitive conclusion from the results in Figure 13 in the 0-200 hours region of the curve. At times greater than 200 hours we can observe a gradual recovery in values of η_o over longer times, with sample B recovering somewhat more than sample A. In contrast, the method based on Halpin-Tsai shows a strong increase in the calculated value of η_o to a level greater than unity, which is physically meaningless since $0 < \eta_o < 1$ by definition. It would therefore appear than the method based on Halpin-Tsai analysis is not suitable for analysis of this type of situation. In overall conclusion of the modulus data we can state that the loss in modulus exhibited by the composite samples can, for the most part, be explained by the plasticisation and swelling of the polyamide matrix by the absorption of the treatment fluid.

The macro-method analysis used here to obtain values of the interfacial shear strength (IFSS) was originally proposed by Bowyer and Bader (26,27) and an improved version has been extensively reviewed by Thomason (28-31). The macro-method has a significant attraction over some other methods in that it utilizes data which are readily available from standard composite mechanical testing and requires only an extra determination of fibre length distribution, which is a common characterisation tool of those working with discontinuous fibre composites. The method is based on the Kelly-Tyson model for the prediction of the strength (σ_{uc}) of a polymer composite reinforced with discrete aligned fibres (32). This model can be simplified to $\sigma_{uc} = \eta_o (X + Y) + Z$, where Z is the matrix contribution, X is the sub-critical fibre contribution, and Y is the super critical contribution, in reference to a critical fibre length defined by $L_c = \sigma_{uf} D / 2\tau$ where σ_{uf} is the fibre strength, D is the average fibre diameter and τ is the IFSS. The Kelly-Tyson model assumes that all the fibres are aligned in the loading direction and the equation cannot be integrated to give a simple numerical orientation factor to account for the average fibre orientation. When the stress at the 1% and 2% strain levels obtained from tensile testing are combined

with the full fibre length distributions used to obtain the averages in Table 1 and applied in the procedure described above we obtain values for the parameters η_o and τ. Due to the lack of data on the matrix samples when conditioning at 150°C we were only able to carry out this analysis on the samples conditioned at 120°C.

The results obtained for η_o for both series using the above analysis are presented in Figure 14 and compared with the orientation parameters obtained using the Cox analysis as presented in Figure 13. The macro-analysis values, which also use input data from mechanical testing, follow a similar trend to those obtained from the Cox analysis of composite modulus. In particular the values obtained for the DaM samples are very close and can be considered to be identical at the 95% confidence level. It is also apparent that the trends lines for the data obtained by the two methods for the conditioned samples follow parallel lines. However, there is also a major difference between the results of the two methods in the initial drop in the value of η_o when going from DaM to conditioned samples. The first literal interpretation of this result would be that the average orientation of the fibres in these samples is changed significantly by the conditioning treatment. It is certainly true that the anisotropic swelling of these samples could actually lead to a slight decrease in the average fibre orientation parameter. However, it is not possible to obtain the kind of physical changes that would be necessary to explain the results in Figure 14, which would require a change from a highly oriented system to one where the fibres are close to a random orientation. The dotted lines in Figure 14 show the level of the fibre orientation parameter as measured by optical analysis of polished cross sections of composites prepared in a previous study using identical materials and methods (4). The upper level represents the value of the average of $< \cos^2(\phi) >$ and the lower value that of $< \cos^4(\phi) >$, where ϕ is the angle subtended between the fibre axis and the primary loading direction. We have previously made numerous comments on inconsistencies in the match between the values obtained by the optical method and those required to match the composite mechanical properties (3-5,29-31). We suggest that the data shown in Figure 14 is an important clue towards a better understanding of the use of these average orientation parameters in modeling composite performance and we are currently exploring how this can lead to an improvement in the macro-method analysis model.

The data obtained for IFSS, the apparent interfacial shear strength, are shown in Figure 15. Once again we need to be careful in interpreting the data in the earlier stages of the conditioning due to the fact that we are not in an equilibrium situation with regard to the distribution of absorbed liquid in the samples, and it is not clear how such non-uniformity will affect the underlying assumptions of the macro-method analysis. Both series show a similar level of approximately 28 MPa in the DaM state, and both show an increase in IFSS in the early stages of the conditioning, although series B increases more than series A. After the initial increase, the IFSS for series B samples remains relatively constant up to 600 hours conditioning and only starts to show a slight decrease at the 1000 hour time. In contrast the IFSS for series A decreases almost linearly with conditioning time after the initial increase. From the moisture absorption data in Figure 6 we know that both series of composites have reached equilibrium absorption levels by approximately 200 hours conditioning at 120°C. We can reasonably assume that any trends observed in the data after that time can be attributed to actual changes in the samples as opposed to non-equilibrium effects. It would therefore appear that the additional additives in the sizing of glass 173X help to maintain an improved level of fibre-matrix interaction as compared to samples

containing 123D. This is in line with the results of single fibre pullout measurements (33) made using the same glass fibres and polyamide 66 resin. The results obtained in those measurements were assumed to represent the IFSS in a system at equilibrium moisture content for 23°C and 50% RH (approximately 2.5%). Values obtained were 30.3 MPa (2.0 MPa 95% confidence interval) for 173X and 22.8 MPa (4.1 MPa 95% confidence interval) for 123D.

We shall be exploring the full consequences of these important discoveries in a future report. The apparent increase in IFSS when going from dry to conditioned samples would seem to be an important clue to a possible discrepancy with the calculation of IFSS using the macro-model. The strong expectation would have been for the level of IFSS to fall since the shear strength of the PA66 matrix calculated from the tensile strength using von Mises criterion falls from 40 MPa for the dry matrix to approximately 20 MPa for the 120°C conditioned matrix. We would not normally expect the apparent IFSS to be higher than the matrix shear strength. However, it also seems likely that the explanation of the step change in orientation factor will provide an explanation for the inconsistencies that we have previously observed between optically measured orientation parameters and the values required to obtain acceptable modeling of the composite performance. There can be little doubt that the IFSS is an important parameter in determining the mechanical performance of glass reinforced thermoplastics. In previous reports we have discussed the relative role that chemical and physical interaction play in the level of apparent IFSS (3, 28-31,34). We have shown that shrinkage stresses contribute significantly to the apparent IFSS in these systems. It seems reasonable to suggest that the level of radial interfacial stress in the glass-polyamide system would be significantly reduced by the swelling due to moisture absorption. If this were the case we should be able to find a correlation between the level of swelling and the mechanical performance of the composites. This hypothesis is examined in Figures 16-17 where we plot mechanical performance against cross sectional swelling for both series at both conditioning temperatures. Examination of these Figures reveals that, in general, there is a strong inverse relationship between mechanical performance and the swelling of the composites due to moisture absorption. Furthermore, it appears possible in most cases to draw a connecting line between the trend lines for any series at the two conditioning temperatures. This would seem to offer the possibility of predicting performance at any conditioning time and temperature from data obtained under different conditions. This is an area which requires further investigation.

Conclusions

This study of injection moulded glass-fibre reinforced polyamide 66 composites has revealed that hydrothermal ageing in water-glycol mixtures results in significant changes in the mechanical performance and dimensions of these materials. Conditioning at 120°C led to a large drop in both composite tensile modulus (-50%) and strength (-50%) within 24 hours. With longer conditioning times, up to 1000 hours, the tensile modulus did not show further major changes, however the composite tensile strength development was shown to be dependent on the glass fibre sizing formulation. Conditioning at 150°C resulted in a more severe negative impact on tensile performance. In particular the composite tensile strength showed no stability after the initial steep loss and continued to decrease with increased conditioning times. These negative effects at 150°C could be mitigated to some degree by the appropriate design of the glass fibre sizing; however the sizing effect diminished with increasing conditioning time (at 150°C). The effects of hydrothermal conditioning on tensile elongation and unnotched impact were more complicated. Conditioning at 120°C led to an increase in the tensile elongation of both composites and PA66 matrix. In the composites it was observed that the level of this increase was dependent on the glass fibre sizing. After an initial increase, the tensile elongation slowly decreased with increasing conditioning time. With conditioning at 150°C there was also evidence of an initial increase in tensile elongation. However, it was also clear that a rapid degradation of tensile elongation was also taking place with increasing conditioning times with a major loss occurring after 96 hours. Up to this time there was also a significant effect of fibre sizing on the tensile elongation of the composites. The trends for composite unnotched Charpy and Izod impact closely follow those of the tensile elongation. However, in contrast to the tensile elongation, the unnotched impact performance of the PA66 resin itself falls sharply (-60%) at short conditioning times, after which it remains fairly constant (for conditioning at 120°C). It was not possible to measure the performance of the resin samples after conditioning at 150°C due to the severe levels of physical degradation.

All materials showed a weight increase due to conditioning at 120°C which was typical of a single Fickian diffusion process. This process was so rapid that the major portion of the absorption process took place in the first 24 hours of exposure. Consequently we were not able to calculate the diffusion coefficients for these systems. It was noted that the presence of the glass fibres reduced the fluid uptake by an amount significantly greater than would be expected from a simple scaling with the resin content of the composites. The composite weight increase for conditioning at 150°C was much greater than at 120°C and there was clear evidence of multiple processes involved over time. After approaching an initial plateau level the weight increase showed evidence of steps upward after 72 hours and a further step up after 600 hours conditioning. The dimensional changes of the samples in both thickness, width, and a calculated cross section closely followed the trends observed for the weight increase. It was not apparent that the glass fibre sizing affected the dimensional stability of the composites. We show that there is a strong correlation between the swelling of these samples and the level of fluid adsorption. Plots of the swelling coefficients for the composite width and thickness show excellent correlation for the data obtained at 120°C and also data obtained at 150°C up to 96 hours conditioning time. The data obtained at longer times at 150°C show some deviation from the linear trend, also

indicative of a second process taking place at these extreme conditions. Although the PA66 resin showed reasonably homogeneous swelling, the composites exhibited different levels of swelling depending on direction. These effects were well in line with the known effects of fibres on restriction of the matrix deformation (mechanical, thermal or moisture swelling) in the fibre direction. These differences can be well correlated with the average fibre orientation with respect to the various direction axes.

We have calculated the average fibre orientation parameters for these systems using various micro-mechanical models and the composite mechanical properties. Although we obtained good agreement with the results of these methods for the dry samples, it was clear that the method based on the Halpin-Tsai approach gave unacceptable values for the fibre orientation in the conditioned composites indicating the unsuitability of the Halpin-Tsai approach for the calculation of an average fibre orientation parameter in this type of composite. Values for the interfacial shear strength in the conditioned composites obtained using the macro-method appeared to be significantly higher than the calculated value of the matrix shear strength. Composite mechanical properties such as tensile strength and unnotched impact resistance appeared to scale inversely with the level of swelling of the material.

Tables

	Glass/System A		Glass/System B	
	Average	95% C.L	Average	95% C.L
Average Fibre Diameter (μm)	10.0	0.89	9.7	1.05
Number Average Length (mm)	0.32	0.03	0.30	0.02
Weight Average Length (mm)	0.53	0.04	0.47	0.03
Glass Weight Content (%)	30.9	0.2	30.7	0.11

Table 1: Fibre and Composite Characterisation

	Swelling Coefficients		
	Width	Thickness	Length
Original Experiments			
PA66 Resin	0.28	0.37	not measured
System A&B	0.38	0.85	not measured
Recent measurements			
PA6,6 Resin	0.29	0.42	0.26
System A Composite	0.33	0.85	0.03

Table 2: Swelling coefficients of moulded PA66 and Composites

References

1. N. Sato, T. Kurauchi, S. Sato, and O. Kamigaito, J. Compos. Mater., **22**, 850 (1998).
2. F. Ularych, M. Sova, J. Vokrouhlecy, B. Turi, Polymer Composites, **14**, 229 (1993)
3. J.L. Thomason, Polymer Composites, **27,** 552 (2006)
4. J.L. Thomason, Polymer Composites, **28**, 331 (2007)
5. B. Mouhmad, A. Imad, N. Benseddiq, S. Benmedakhène and A. Maazouz, Polymer Testing, **25**, 544 (2006)
6. E.Carlson and K. Nelson, Automotive Engineering, **104**, 84 (1996)
7. D.Valentin, F.Paray, and B.Guetta, J.Mater.Sci., **22**, 46 (1987)
8. Z.A. Mohd Ishak and J.P. Berry, J.Appl.Polym.Sci., **54**, 2145 (1991
9. M. Akay, J.G. Cracknell and H.A. Farnham, Polymers & Polymer Composites, **2**, 349 (1994)
10. N. Takeda, D. ZY. Song, K, Nakata, Adv. Composite Mater. **5**, 201 (1996)
11. A.Bergeret, I.Pires, M.P.Foulc, B.Abadie, L.Ferry, and A.Crespy, Polymer Testing **20**, 753 (2001)
12. N. Jia, H.A.Fraenkel and V.A. Kagan, J.Reinforced Plastics and Composites, **23**, 729 (2004)
13. I. Carrascal, J.A. Casado, J.A. Polanco, F. Gutiérrez-Solana, Polymer Composites, **26**, 580 (2005)
14. T.A. Coakley, J.E. Rubadue, C.E. Forman and R.A. Schweizer, United States Patent 4,255,317 (1981)
15. J.L. Thomason and L.J. Adzima, Composites Part A **32**, 313 (2001).
16. M.Cossement, N. Masson and W. Piret, United States Patent 5,236,982 (1993)
17. N. Masson, J.M. Henrion, J.L. Thomason, L.J. Adzima, T.L. Cheney, W.Piret, M. Cossement, United States Patent 6,365,272 (2002)
18. J.Crank and G.S.Park (eds) Diffusion in Polymers, Academic Press, New York, 1968
19. J.L.Thomason, Composites **26**, 477 (1995)
20. B.W.Rosen in Engineered Materials Handbook, Volume 1 Composites, ASM International, 1987
21. R.A.Schapery, J.Composite Materials **2**, 380 (1968)
22. J.L.Thomason and W.M.Groenewoud, Composites Part A **27A**, 555 (1996)
23. J.L. Thomason, submitted to Polymer Composites 2006
24. H.L. Cox, Brit.J.Appl.Phys. **3**, 72 (1952)
25. J.C. Halpin and J.L. Kardos, Polym.Eng.Sci. **16**, 344 (1976)
26. M.G. Bader and W.H. Bowyer, Composites **4**, 150 (1973)
27. W.H. Bowyer and M.G. Bader, J. Mater. Sci., **7**, 1315 (1972)
28. J.L.Thomason, Composites Part A **33**, 1283 (2002).
29. J.L.Thomason, Compos.Sci.Technol. **62**, 1455 (2002).
30. J.L.Thomason, Composites Part A **33**, 331 (2002).
31. J.L.Thomason, Compos.Sci.Technol., **61,** 2007 (2001)
32. A. Kelly and W.R. Tyson, J.Mech.Phys.Solids, **13**, 329 (1965)
33. J.L.Thomason and G.Kalinka, Composites Part A **33**, 85 (2001).
34. J.L.Thomason, Composites Part A **38**, 210 (2007).

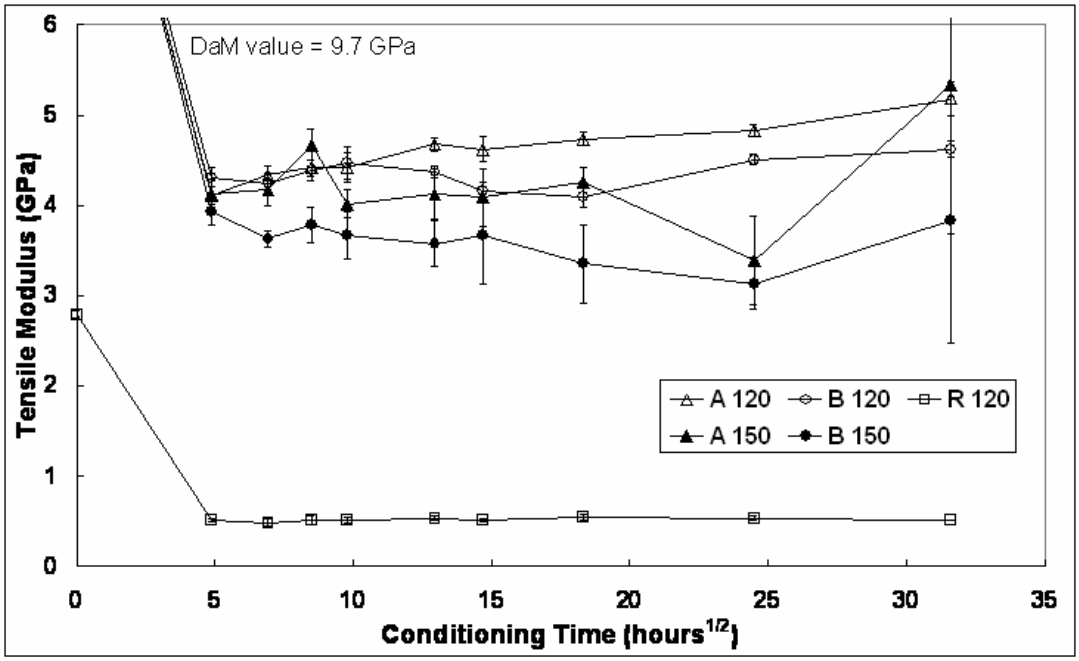

Figure 1 Tensile Modulus vs Conditioning Time

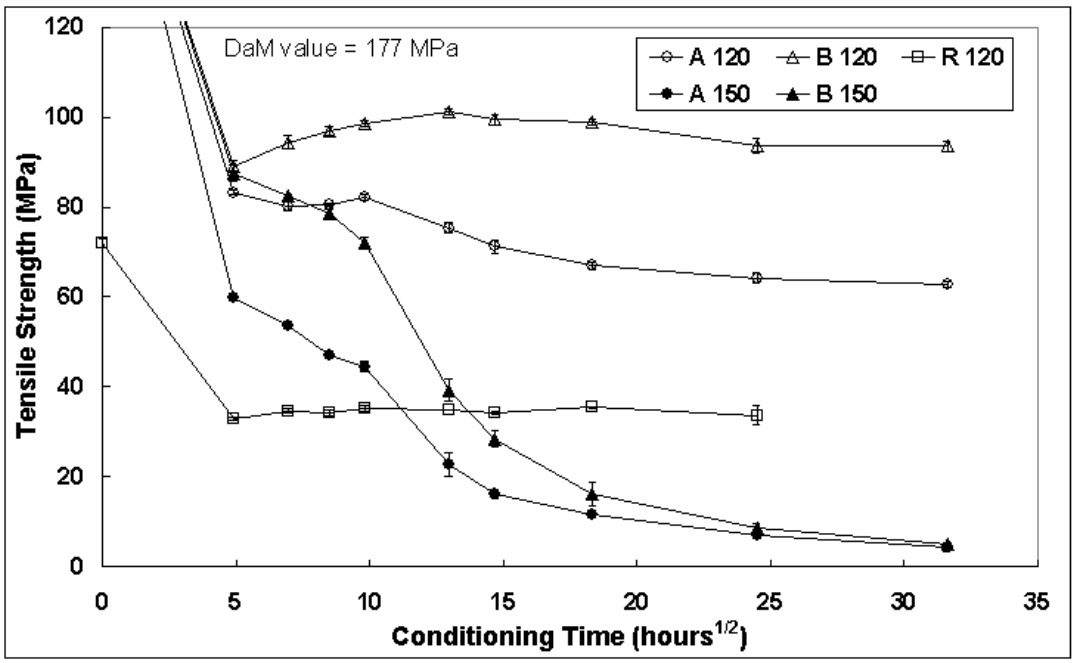

Figure 2 Tensile Strength vs Conditioning Time

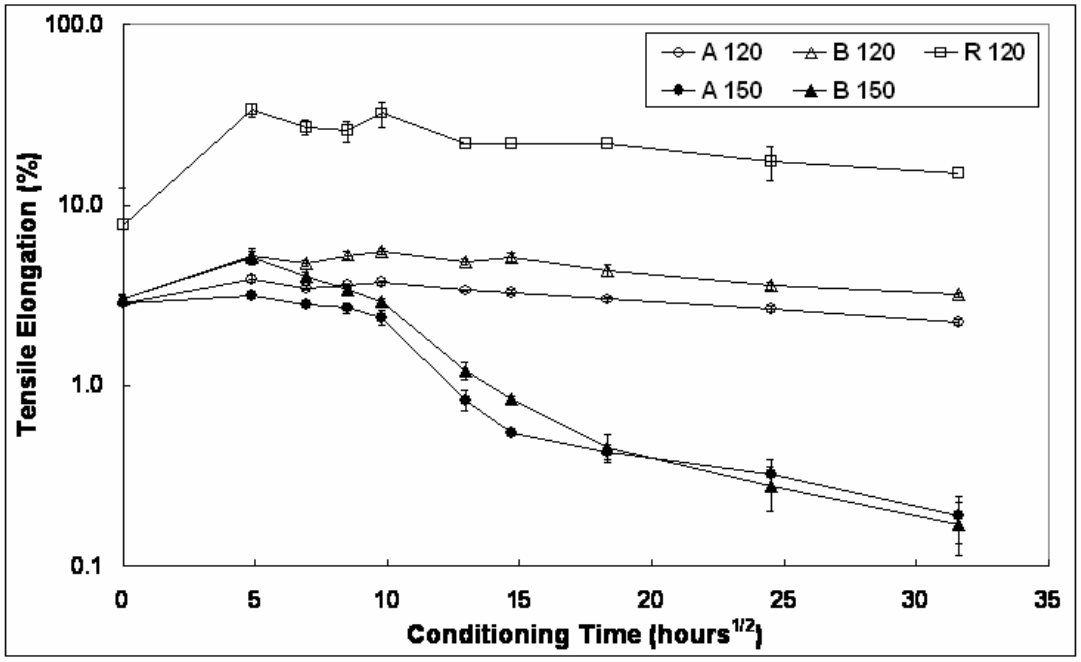

Figure 3 Tensile Elongation vs Conditioning Time

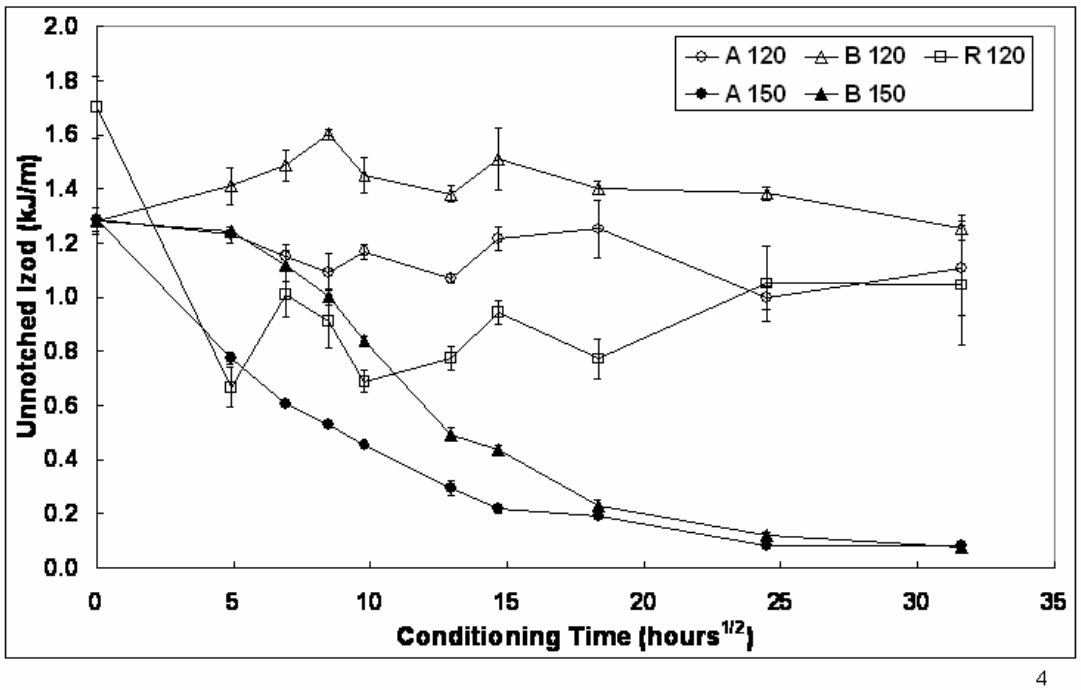

Figure 4 Unnotched Izod Impact vs Conditioning Time

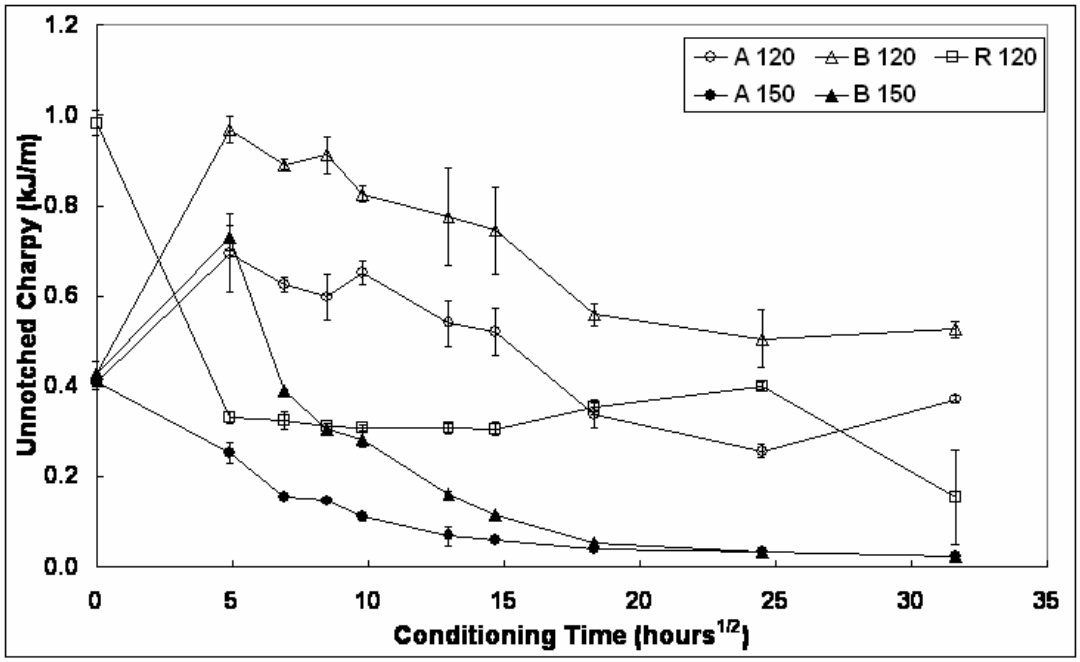

Figure 5 Unnotched Charpy Impact vs Conditioning Time

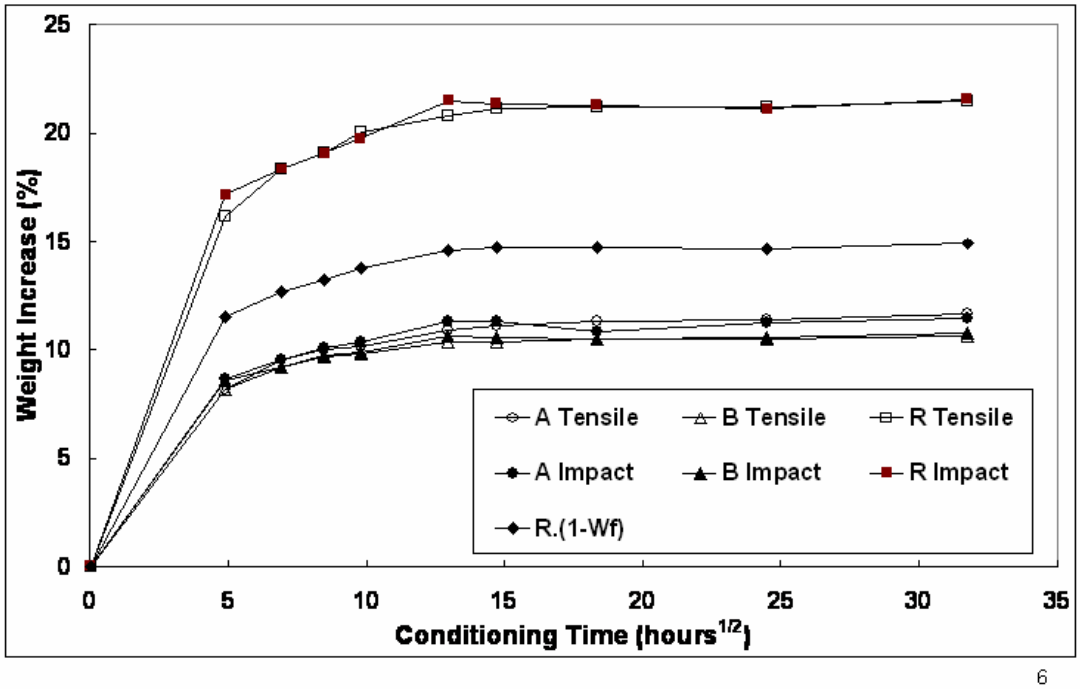

6

Figure 6 Weight Increase vs Conditioning Time at 120°C

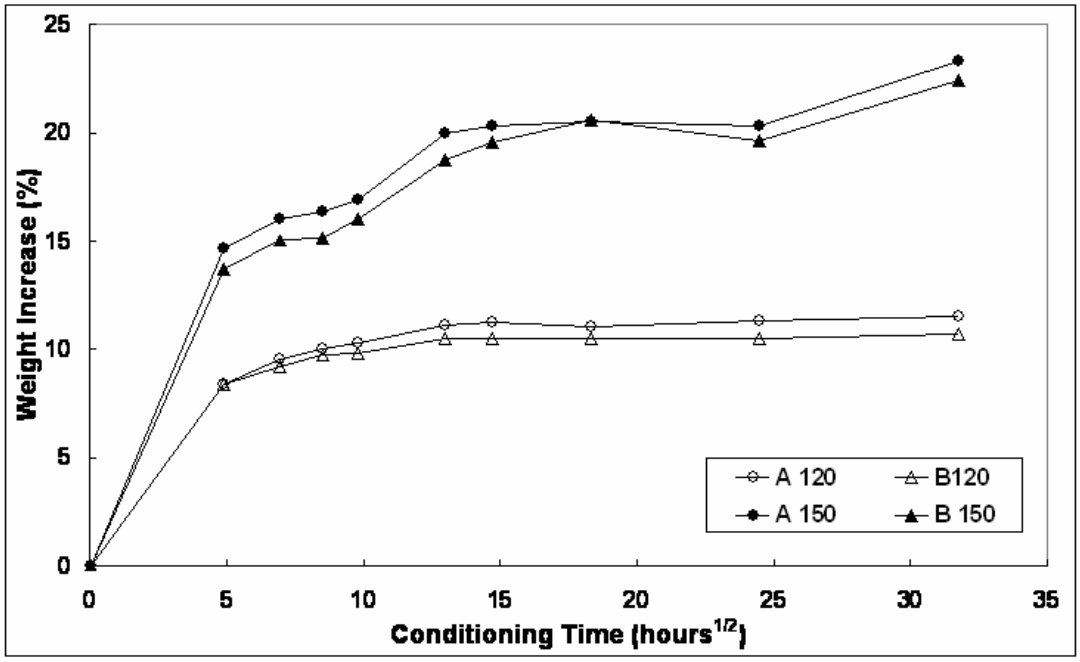

Figure 7 Weight Increase vs Conditioning Time at 120°C and 150°C

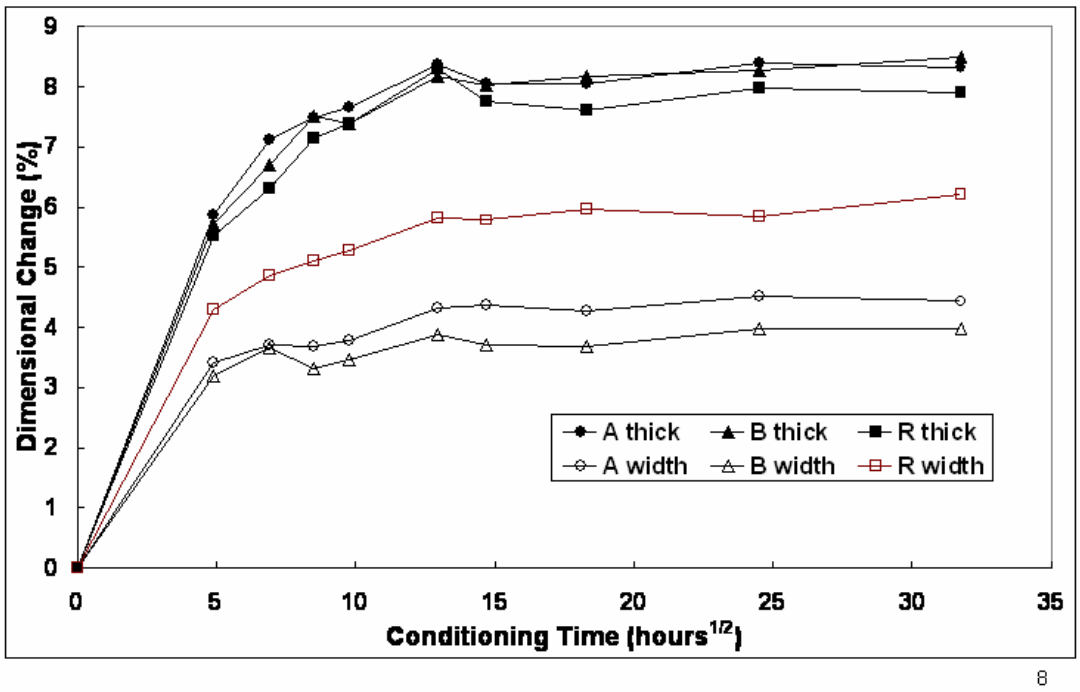

Figure 8 Dimensional Change vs Conditioning Time at 120°C

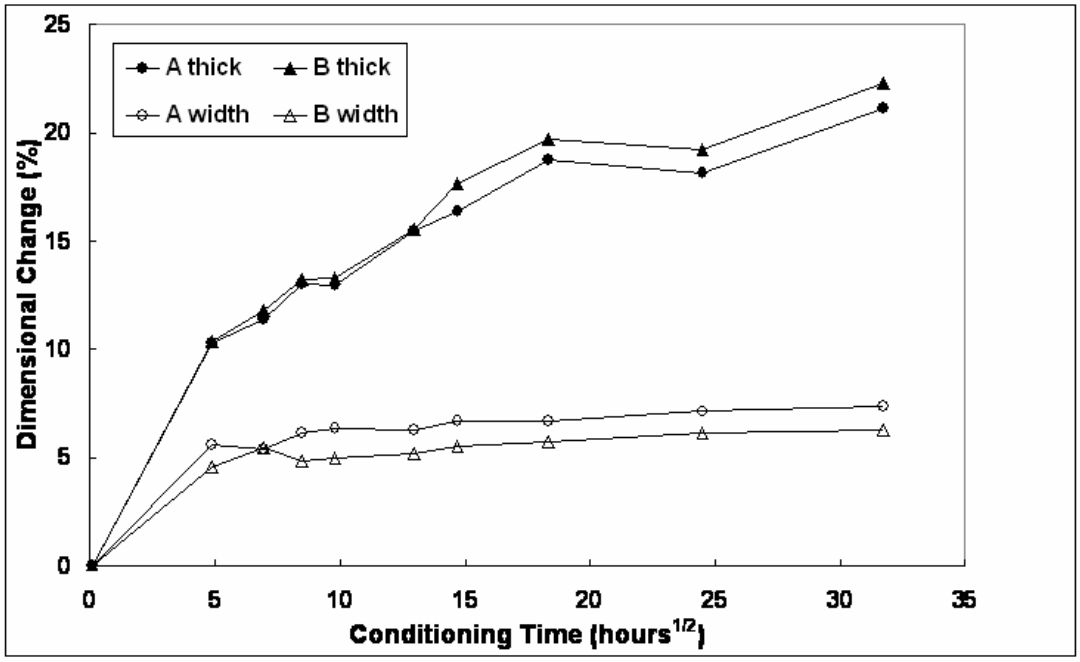

9

Figure 9 Dimensional Change vs Conditioning Time at 150°C

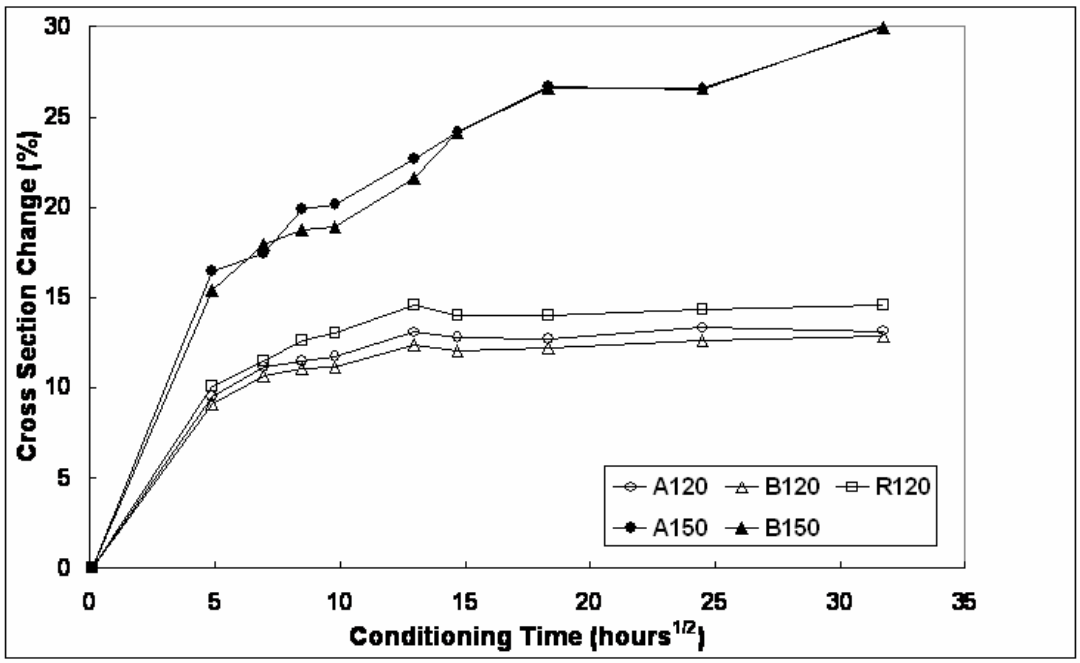

10

Figure 10 Cross Sectional Change vs Conditioning Time at 120°C and 150°C

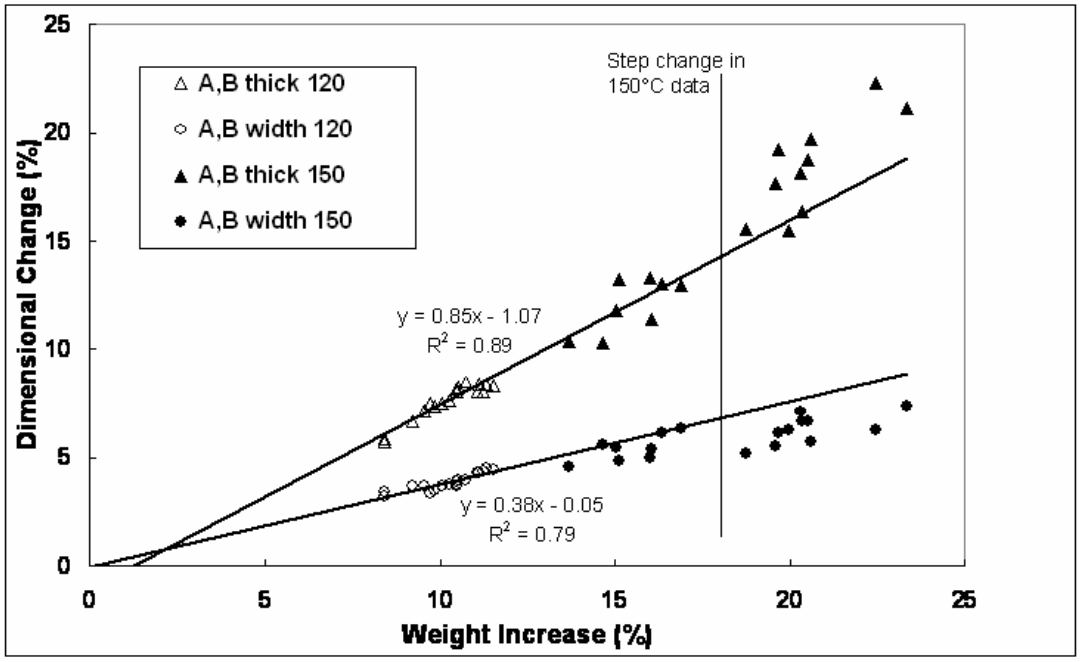

11

Figure 11 Dimensional Change vs Weight Increase

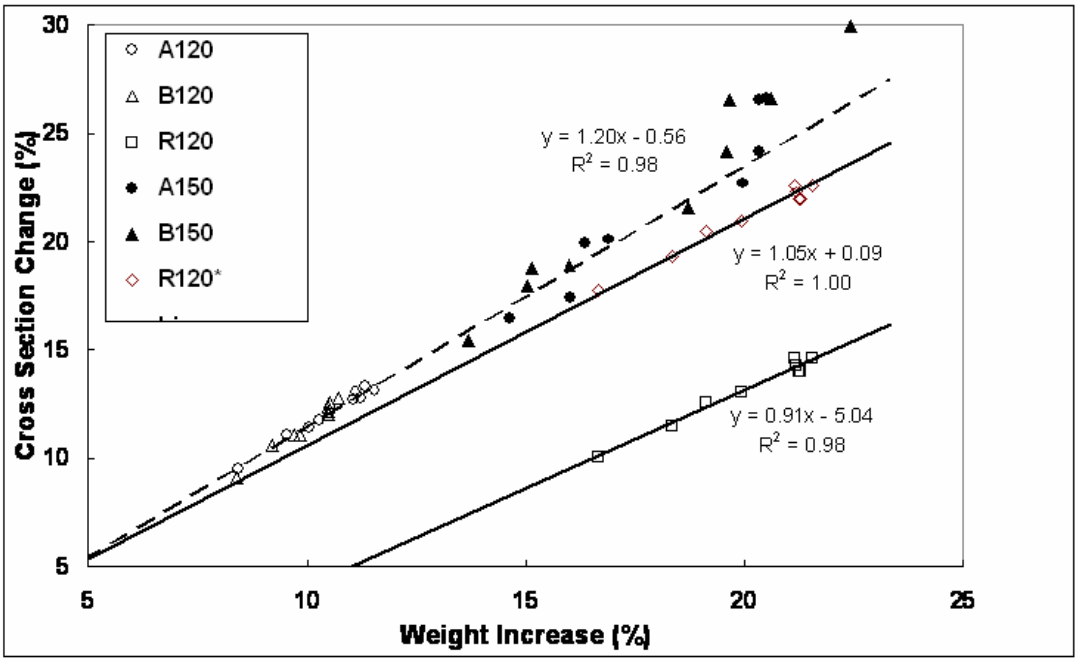

12

Figure 12 Cross Sectional Change vs Weight Increase

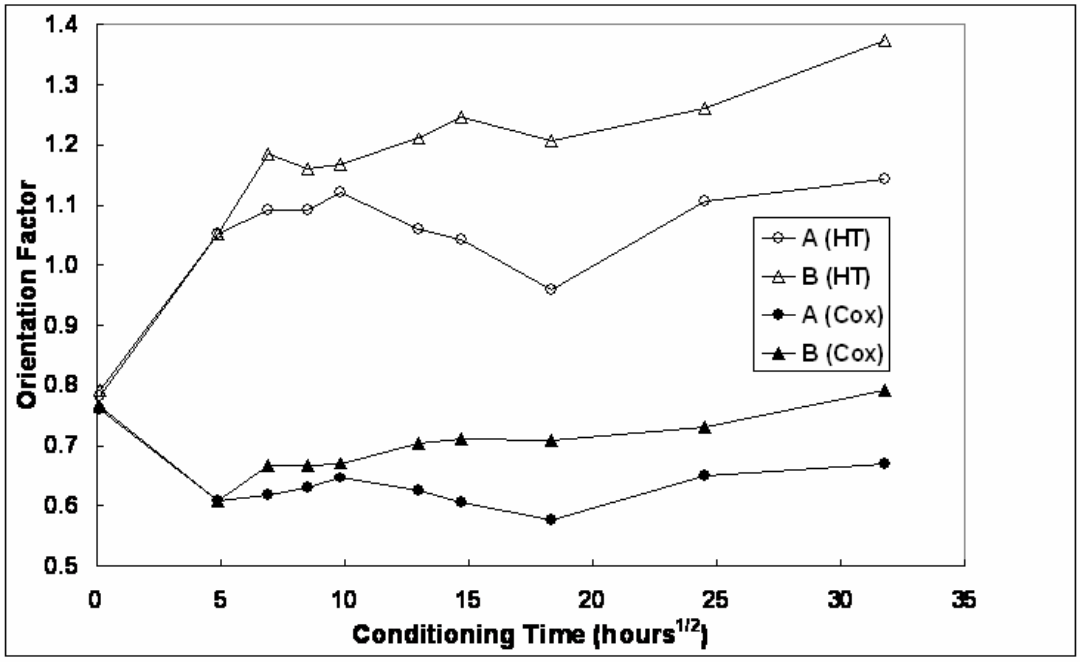

Figure13 Calculated Average Fibre Orientation Factor vs Conditioning Time at 120°C

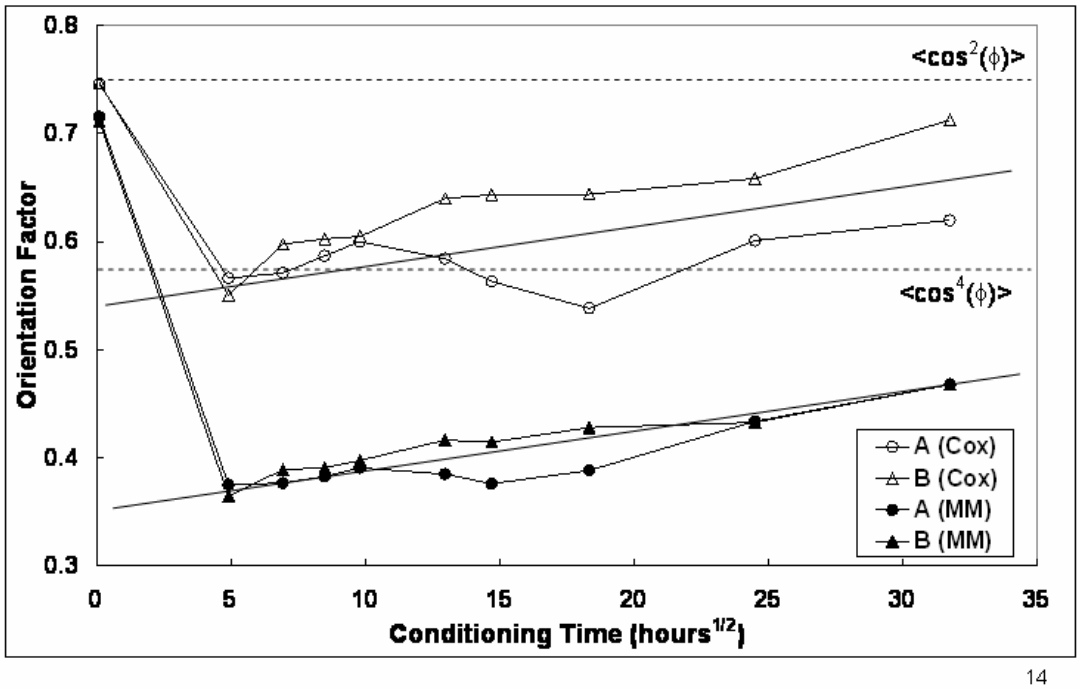

Figure14 Macromethod Average Fibre Orientation Factor vs Conditioning Time at 120°C

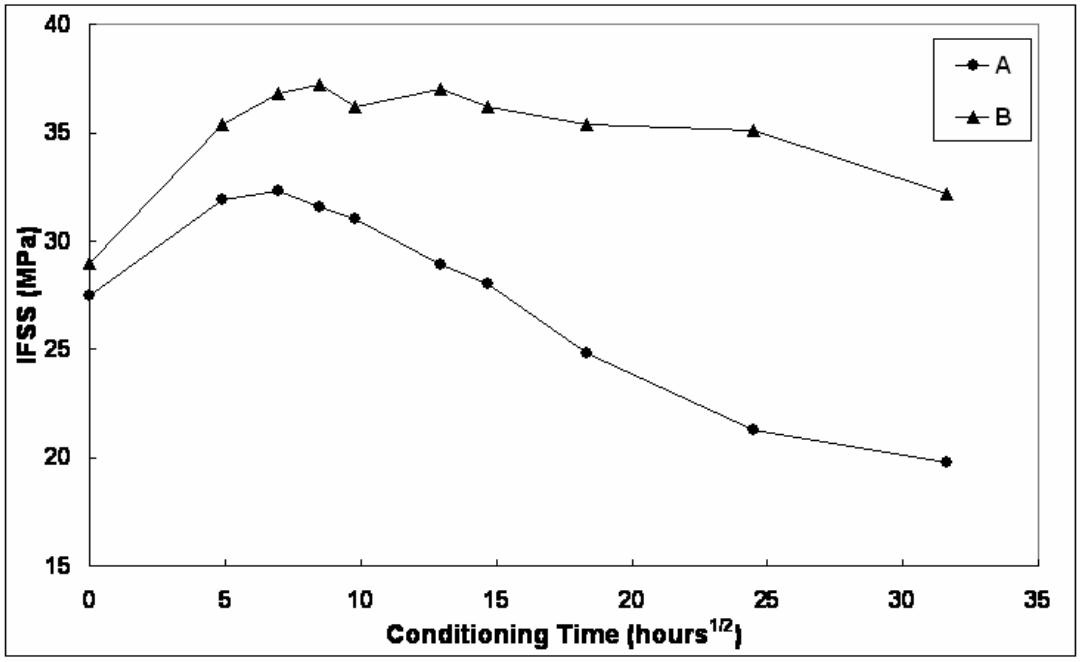

Figure15 Macromethod Calculated IFSS vs Conditioning Time at 120°C

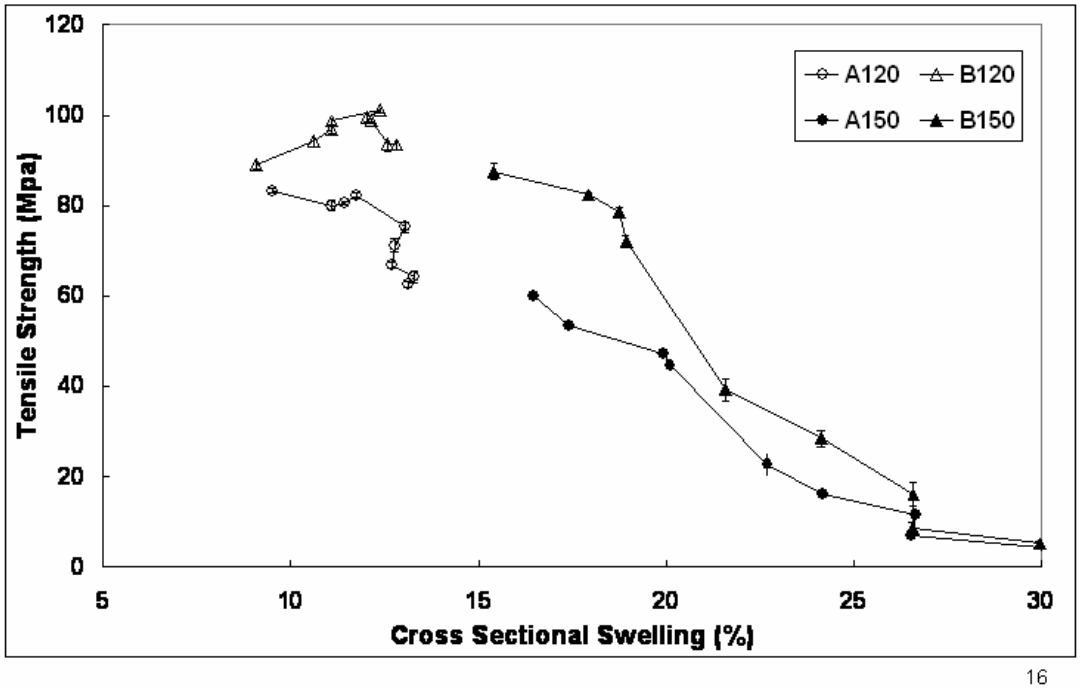

Figure 16 Tensile Strength vs Cross Sectional Swelling

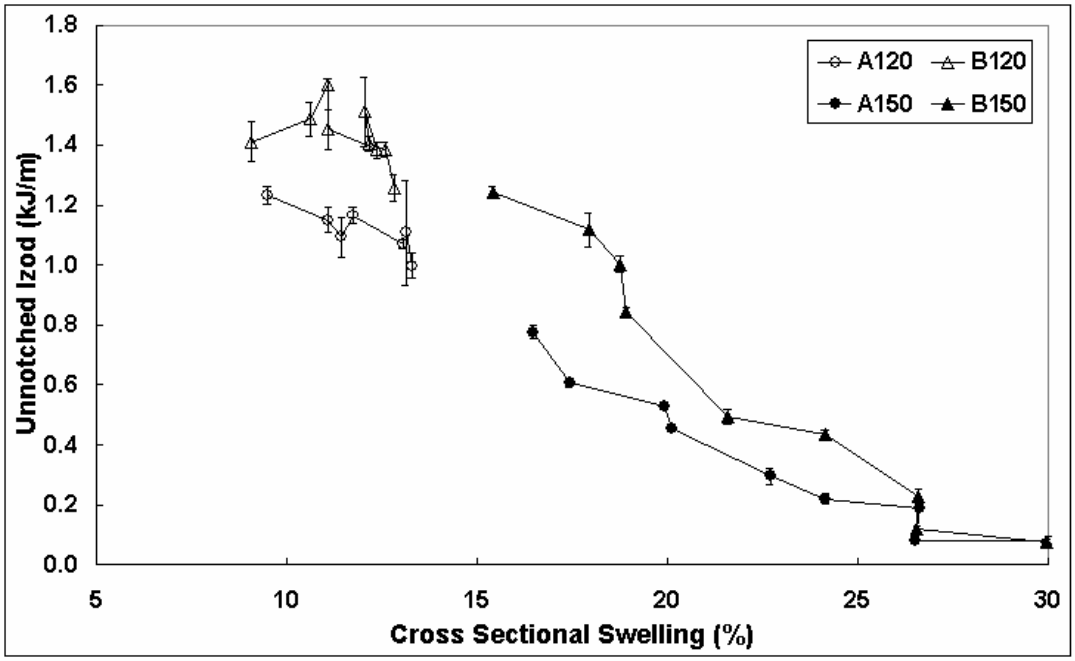

Figure 17 Unnotched Izod Impact vs Cross Sectional Swelling